We are IntechOpen, the world's leading publisher of Open Access books Built by scientists, for scientists

4,800
Open access books available

122,000
International authors and editors

135M
Downloads

Our authors are among the

154
Countries delivered to

TOP 1%
most cited scientists

12.2%
Contributors from top 500 universities

CLARIVATE ANALYTICS BOOK CITATION INDEX INDEXED

WEB OF SCIENCE™

Selection of our books indexed in the Book Citation Index in Web of Science™ Core Collection (BKCI)

Interested in publishing with us?
Contact book.department@intechopen.com

Numbers displayed above are based on latest data collected.
For more information visit www.intechopen.com

Chapter 6

Monitoring of the Surface Modification of Nanoparticlesby Electrochemical Measurements Using Scanning Electrochemical Microscope

David Hynek, Michal Zurek, Petr Babula,
Vojtech Adam and Rene Kizek

Additional information is available at the end of the chapter

http://dx.doi.org/10.5772/57203

1. Introduction

1.1. SECM as a tool for multi-purpose characterisation of materials

The first papers related to the scanning electrochemical microscopy (SECM) were published in the nineties of the 20th century [1, 2]. This technique is based on the scanning of the studied surface by ultramicroelectrode (UME) and electrochemical analysis of surface [1]. Such technique gives us an electrochemical picture of the surface. SECM employs an UME probe (tip) to induce chemical changes and collect electrochemical information while approaching or scanning the surface of interest (substrate). The substrate may also be biased and serves as the second working electrode. Many different types of UMEs have been fabricated, e.g., microband electrodes, cylindrical electrodes, microrings, disk-shaped, and hemispherical electrodes [3]. The disk geometry of the UME is the most preferred design from many reasons discussed below. UME is the most important part of the electrochemical microscope, which determines the results of scanning. Electrodes in micro or nano dimensions offer important advantages for electroanalytical applications including greatly diminished ohmic potential drop in solution and double-layer charging current, the ability to reach a steady state in seconds or milliseconds, and a small size allowing make experiments in microscopic dimensions [4].

SECM requires minimal sample preparation than other spectroscopy techniques (e.g. fluorescence or electron microscopy). Another advantage is that the evaluation of image outputs can be numerically modelled, allowing to obtain information and analysis the reaction kinetics.

Therefore, it is possible to study effectively both material characteristic and biological properties [4]. Due to the non-destructive measurement method, experiments can be successfully repeated several times. The SECM surface scanning is connected with one major risk of damage to the scanning electrodes or the studied surface due to distance between the tip and surface interference. This distance should be optimized and the probe or a tip should be held at a constant height above the surface during measurement. Analysed surface can act as a second working electrode and therefore four electrodes configuration is used in SECM [5].

Application of SECM is very wide and allows studying various structures and processes in micro and submicrometer-sized systems [5-7]. The target of detection could be electron, ion, and molecule transfers, and other reactions at solid-liquid, liquid–liquid, and liquid-air interfaces. In recent years the study of nanoparticles and its application rapidly has been increasing [8]. The SECM study of nanoparticles increases rapidly too because the surface modification by this nanoparticles brings many positives and allows to open the whole new research area [8]. The wide range of SECM applications allows to investigate a wide variety of processes, corrosion of metals, characterization of materials, membrane and enzymatic reactions, photosynthesis, DNA hybridization and metabolism in single living cells [4]. This direction has had the great influence for the increase of published papers related to the SECM technique since the year 1995 (approximately) [2]. The bio-applications of SECM are one of the most developed areas in the recent years and the usage of nanoparticles in this area is very widespread [4, 8, 9].

1.2. Measuring modes and principles of SECM

Although the theory of SECM measurements has been described in many books and reviews, we still consider beneficial to present here the short overview of this. At first, Figure 1 shows a schematic diagram of the basic SECM instrument. An UME tip is attached to a 3D piezo positioner controlled by a computer, which is also used for data acquisition. A bi-potentiostat controls the potentials of the tip and/or the substrate versus the reference electrode and measured tip and substrate currents are in pA and sub-pA orders. 10 pA is the lowest detectable current, the maximum is at 250 mA. Measured current resolution is 0.0015% of current range (minimum 0.3 fA). These informations are related to the model ChInstrument 920D which is shown on Figure 2. Usually detected currents are in pico or nano amper order. The most SECM measurements take place in feedback (FB) or generation/collection (GC) modes [4, 10, 11].

The feedback mode usually uses the ultramicroelectrode (UME), which serves as a working electrode in a three or four-electrode system. The four electrode system is completed with a sample (substrate) that serves as a second working electrode. The electrodes are immersed in a solution containing redox mediator. Specifically, one redox form of a quasi-reversible redox couple. In the following discussion it is assumed that the reduced form R is added, although the same explanations hold for the addition of the oxidized form O of the mediator if the reaction directions are reversed.

http://dx.doi.org/10.5772/57203

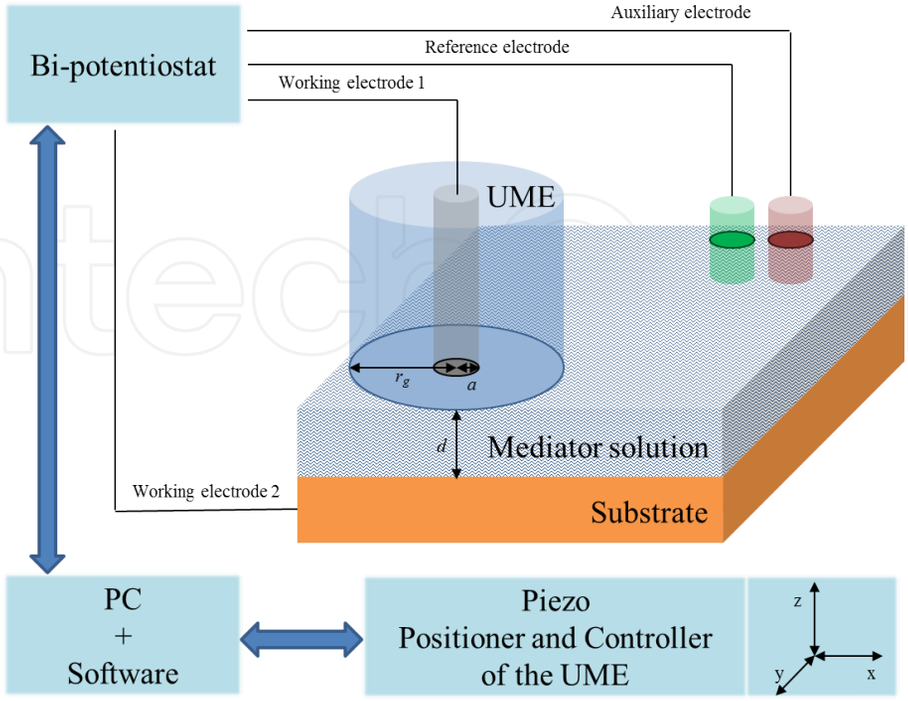

Figure 1. Scheme of SECM instrumentation. The basic parts are as follows: a piezo positioner and a controller of the UME, a bi-potentiostat and PC (with measuring software). The UME scans the substrate surface due to moving the UME by the piezo positioner. The system can work in a three- or four-electrode setup (with connected second working electrode).

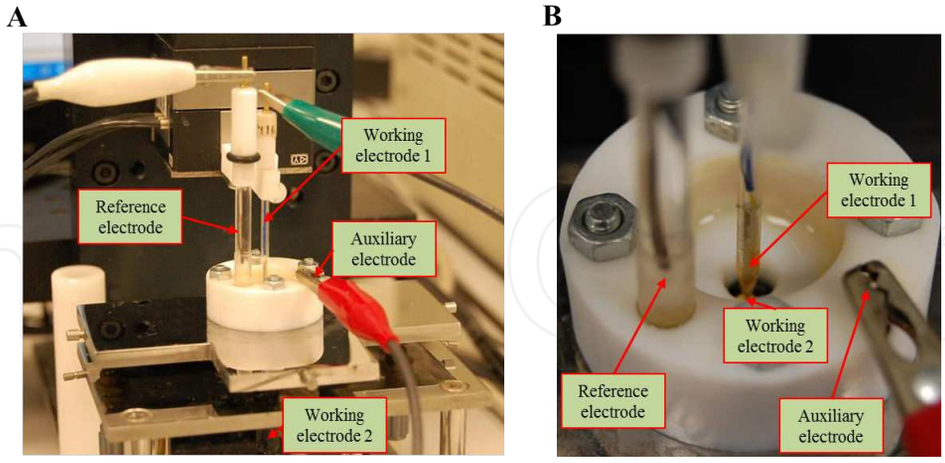

Figure 2. Real picture of measurement apparatus ChInstruments 920D. (A) The overview of the whole electrochemical cell with support. (B) The detail image of the electrochemical cell with connected electrodes.

In the simplest case, the UME is inserted only in mediator solution, a potential is applied to the tip, and diffusion-controlled conversion of the mediator occurs according to equation as it follows:

$$R \rightarrow O + ne^- \quad (1)$$

and thus a steady-state faradaic current $i_{T\infty}$ could be detected. This situation is necessary to understand as the limiting case where the distance d of the tip from the substrate electrode is infinite (Fig 3A). If the UME is in proximity with substrate electrode and this is an insulator, the surface hinders the diffusion of R towards the UME (Fig 3B) and the faradaic current i_T decreases. Such situation is named as a negative feedback. The opposite situation is the positive feedback, which differs by conducting substrate where heterogeneous reaction takes place. This reaction regenerates the R by electrochemical conversion and thus the new reagent source becomes available (Fig 3C). From this reason i_T increases, especially with respect to the dependence i_T (d) [2, 5, 12].

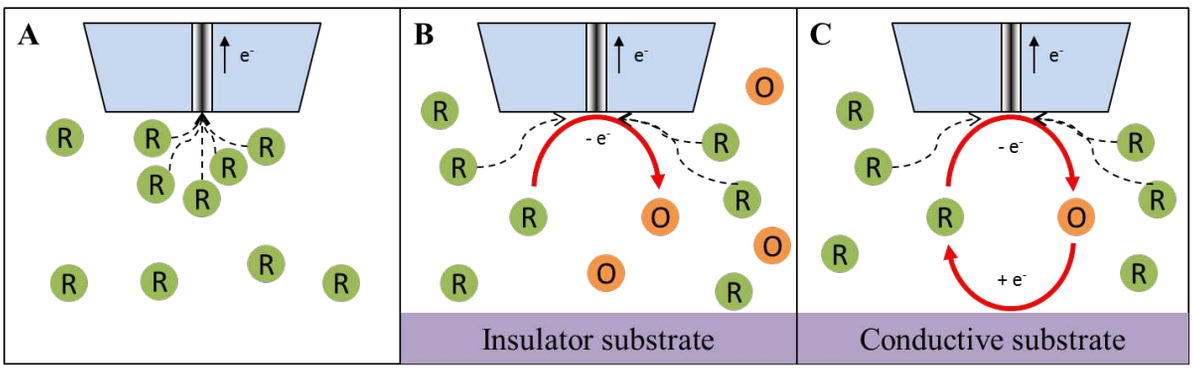

Figure 3. Scheme of feedback mode of the SECM operation. (A) The UME tip is far from the substrate and the tip reaction is caused just form species R from the solution. (B) Negative feedback: the insulating substrate averts the regeneration of species O and diffusion of R to the tip. (C) Positive feedback: species R is regenerated at the substrate and the electrochemical loop is closed.

Generation/collection mode differs from feedback mode in one important thing, the presence of the mediator is solution. This mode works in a solution that does not initially contain any substance that can be converted at the UME at a potential E_T. In the generation/collection (G/C) mode, both tip and substrate can be used as working electrodes. One working electrode generates some species, which are collected at the other electrode. The G/C mode is more sensitive because the background signal is very weak [2, 12].

If an oxidizable or reducible substance is formed on the surface of substrate, this compound can be detected at the UME if it is located close to the active region (Fig 4A). From such description it is obvious the name of the mode, sample-generation/tip-collection (SG/TC) mode. When the tip is moved through the thick diffusion layer produced by the substrate, the changes in i_T reflect local variations of concentrations of redox species. The collection efficiency in SG/TC mode is much lower than that in the TG/SC mode, and the true steady state can be achieved only by using a micrometer-sized substrate. Other disadvantages of this mode are the high sensitivity to noise and the difficulty in controlling the tip/substrate separation distance [2, 12].

http://dx.doi.org/10.5772/57203

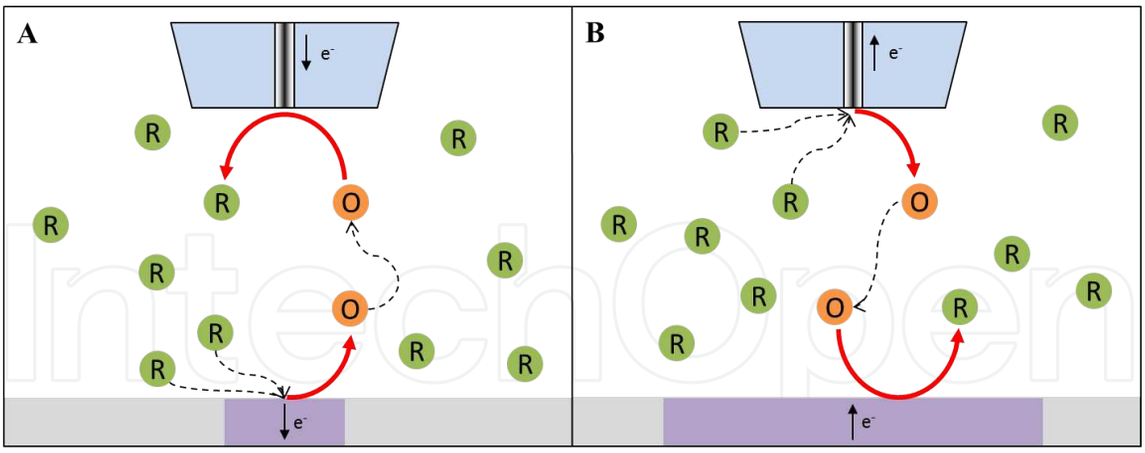

Figure 4. Scheme of SG/TC mode (A) and TG/SC mode (B). (A) O is electrogenerated on the substrate surface and collected at the tip. The tip and substrate currents are recorded in both cases. (B) The tip generates species O by oxidation of R in solution; O diffuses toward the substrate and is reduced back to R.

The application of the contrary processes leads to the creation of the tip-generation/sample-collection (TG/SC) (Fig 4B). In the TG/SC mode experiments, the tip generates an electro-active species that diffuses across the tip/substrate gap to react on the surface of substrate. A TG/SC experiment includes simultaneous measurements of both tip and substrate currents (i_T and i_S). For a one-step heterogeneous electron transfer (ET) reaction at steady state, these quantities are almost identical if d is not very large. Under these conditions, the tip-generated species R predominantly diffuse to the large substrate, rather than escape from the tip-substrate gap. For a process with a coupled homogeneous chemical reaction, there may be large differences between i_S and i_T. If the reaction is slow, the process is diffusion-controlled, and $i_s/i_T \rightarrow 1$ at short separation distances. For the other hand if homogeneous reaction is very fast, most species R get converted to the electro-inactive product before reaching the substrate and hence, the very low substrate current is detected, $i_s/i_T \rightarrow 0$. Between these two extremes, the homogeneous kinetics can be determined by measuring the collection efficiency as a function of d.

As it is obvious in analytical chemistry, connection of various analytical methods to the one sample detection is very popular. Combination of methods allows the new view on the samples. SECM does not stand out of this direction. Studying of surface structures and dynamics is possible due to combination of SECM with other analytical methods. A number of analytical techniques have been combined with SECM [2, 7, 9, 11-17] including near-field scanning optical microscopy (NSOM), surface plasmon resonance (SPR), electrochemical quartz crystal microbalance (EQCM), fluorescence spectroscopy (FS), electrogenerated chemiluminescence (ECL), electrochemical scanning tunnelling microscopy (ESTM) and atomic force microscopy (AFM) [2]. Among above mentioned methods there are two last which would be useful to describe more. Scanning tunnelling microscopy (STM) is based on the concept of quantum tunnelling. When a conducting tip is brought very near to the surface to be examined, a bias (voltage difference) applied between the two can allow electrons to tunnel through the vacuum between them. The resulting tunnelling current is a function of tip position, applied voltage, and the local density of states of the sample [18, 19]. The extension

of STM with electrochemical detection leads to the electrochemical scanning tunnelling microscopy (ESTM) as a powerful new technique for detailed structural and topographical characterization of electrode/electrolyte interfaces. Knowledge of surface structures could be crucial to the understanding of electrochemical processes that are taking place at the electrode surface [18, 19].

Opposite this, the most widely used hybrid method is AFM-SECM. The atomic force microscope maps the topography of a substrate with nanometer vertical resolution by monitoring the interaction force between the sample and a sharp tip, which is attached to the end of a cantilever. AFM methodology is often used to provide a feedback mechanism for height control in scanning near-field optical microscopy. For samples that show variations in both reactivity and topography, it is difficult to resolve these two components with conventional SECM fixed height measurements. The strength of the AFM-SECM combination is in its positioning capabilities and simultaneous possibility of electrochemical detection [20]. Using the AFM mode, one can position a submicrometer-sized tip near the substrate surface and keep a constant tip-substrate distance during the surface raster. Maintaining a constant distance between the tip and the substrate is essential for avoiding tip crashes and the damage to sample during the imaging of a substrate with non-uniform surface reactivity and/or complex topography.

2. Modification of gold electrode

2.1. Self-Assembled Monolayer (SAM)

Self-assembled monolayers (SAMs) are highly ordered molecular assemblies formed by the adsorption of an active surfactant on a solid surface. Understanding and controlling long-range electron transfer across such molecular assemblies are important for the development of technological systems such as molecular electronics and sensors. The most common SAMs are n-alkanethiols adsorbed on gold by Au–S linkage. The manipulation of individual alkanethiolate by SECM [15] is mainly based on regeneration of a gold surface either by electrochemically initiated removal of the chemisorbed thiolate from the gold surface (Eq. 2) or by oxidative decomposition (Eq. 3).

$$AuSR + e^- \longrightarrow Au0 + RS^- \tag{2}$$

$$AuSR + 2H_2O \longrightarrow Au0 + RSO_2^- + 3e^- + 4H^+ \tag{3}$$

The way of preparing the SAMs on metal surface is an immersion of freshly prepared or clean metal electrodes into a dilute solution of alkanethiols for several hours at room temperature. Many authors deal with the optimization of this procedure related to the best reproducibility of the produced SAMs [21]. The most frequently studied alkanethiol compounds with different

http://dx.doi.org/10.5772/57203

features presented in literature are as it follows: n-alkanethiol; α,ω-alkanedithiol; ω-mercaptoalkanol; ω-mercaptoalkane carboxylic acid; ω-mercaptoalkane amino acid [22]. Application of other types of thiols such as aromatic compounds is possible too [22]. Because the metal–sulphur bond is stable between thiols and metal surface, the way for the modification of metal surfaces with organic monolayers could be easily modified with any particular molecule that is firstly thiol-derived and then attached to the metal surface [23].

The formation of a SAM is often depicted in schemes as uniformly aligned molecules on a flat surface. However, it has been recognized that a wide variety of defects are possible such as pinholes, collapsed sites, islands, and domains [24]. Typically, the first assumption is that the metallic surface, upon which the SAM is formed, is uniformly flat. Scanning techniques show a variety of features such as terraces, steps, and crystalline boundaries. The choice of electrode metal is an important factor in determining the SAM integrity. A second assumption is that the organic molecules of the SAM align uniformly. The tilt angle of alkane thiols can cause significant variation in the monolayer packing [25].

SECM has almost been used for studying the structure of alkane thiols, because SECM signals respond very sensitively to defects in the monolayer. A defect-free monolayer passivates the gold electrode so strongly that it behaves like an insulator in SECM. No passivation occurs at defects, and results as high currents. Application of nanometer-sized electrodes showed that direct electron transfer through the layer, rather than electron transfer at the defects, was dominant and the size of the defects was 1–100 nm [26].

Model for electron transfer at self-assembled monolayers measured by scanning electrochemical microscopy has been suggested by *Liu and Bard, et al.* [27]. The developed models were used to measure independently the electron transfer rates mediated by monolayer-attached redox moieties and a direct electron transfer through the film as well as the rate of a bimolecular electron transfer reaction between the attached and dissolved redox species.

When the monolayer absorbed on the substrate contains an electroactive group, the regeneration of the mediator occurs via a bimolecular reaction with these surface-bound redox centres with a rate constant k_{BI}. The rate of the tunnelling ET is governed by the relative contributions from the forward and backward reactions, k_f and k_b, which are both dependent on the value of substrate potential E_s. If bimolecular ET reaction is irreversible and the electron tunnelling through the monolayer is quasi-reversible, the effective rate constant obtained from fitting an experimental approach curve to theory is k_{eff}. After some approximations and limited conditions presented in [17] the one important result is formed as follows: the concentration and potential will not affect k_{eff} and the overall rate of ET is limited by the bimolecular ET rate constant, k_{BI}.

Forming of SAMs on the surface of substrate electrode is one of the most applied procedures in SECM techniques. The great advance of this lies in the immobilisation of target molecules and possibility of creating the surface electrochemical image. Application of SAMs systems in SECM measurements have many utilizations as the study of electron transfer through the creating monolayer [27-32], investigation of various functionalizations of the SAMs parts [33,

34], monitoring the adsorption/desorption processes [35, 36] and interactions between monolayer and target molecules [37].

2.2. Paramagnetic particles

Paramagnetic particles are usually used as an isolation tool in biological applications [38]. Its specificity is related with the paramagnetic properties of the metal core, which reacts on external magnetic field and the other specificity is caused by the surface modification. Connection of SECM detection with nanoparticles, in general, leads to the generation of the one basic problem. What is the measured signal? It is the signal of individual particles, or the average signal of the layer? The most application leads to the second variant. However, some authors focused on the detection of single particle [8]. *Quinn et al.* [39] reported one of the first uses of SECM to investigate the properties of metal NPs. They followed the compression of a monolayer of monodisperse thiol-capped AgNPs as the investigating of NP-film conductivity changes with particle interdistance. *Tel-Vered and Bard* [40] used SECM for the first time to synthesize and to characterize a single particle on a conductive carbon support. Using this approach, they avoided the problems arising from multi-NP synthesis (e.g., narrow size distribution, surface agglomeration, occurrence of lattice defects, and poisoning of the metal by impurities).

Usage of paramagnetic particles in SECM techniques is focused on the improvement of the binding of bio-compound(s) (enzymes, antibodies, etc.) onto the electrode surface [8]. Direct connection of bio-compounds with electrode surface is very often disrupted by many phenomena as follows: loss of biochemical activity, nonspecific binding, blocking of the electrode surface, and regeneration of the sensing surface [41]. Application of paramagnetic particles onto the electrode surface with subsequent SECM detection has been presented by some authors as it follows.

Wijayawardhana, C. A. and Wittstock, G. et al. [41, 42] present miniaturized sandwich enzyme immunoassay for the model analyte mouse-IgG. After capturing mouse IgG by the primary anti-IgG antibody (Ab) coupled with magnetic particles, a second anti-IgG Ab conjugated to an enzyme-label (alkaline phosphatase – ALP) is bound to the analyte. ALP catalyses the hydrolysis of 4-aminophenyl phosphate (PAAP). Platinum microelectrode scans surface over the beads domains and detect product of hydrolysis, 4-aminophenol, by oxidation. The scheme is presented in Fig. 5.

The other Wittstock's cooperation, this time with *Zhao C.* [43, 44], was focused on the system based on the activity of glucose dehydrogenase (GDH). This enzyme was chosen because of its high activity and independence of dissolved oxygen in the sample catalysing the transfer of electrons from glucose to an electron mediator. Biotinylated glucose dehydrogenase was bound to streptavidin-coated paramagnetic beads, which were located on a hydrophobic surface. The catalytic activity of immobilized GDH was mapped in SECM feedback mode and generation-collection mode using ferrocenemethanol, ferrocenecarboxylic acid, *p*-aminophenol, and ferricyanide as electron mediators, respectively [44].

http://dx.doi.org/10.5772/57203

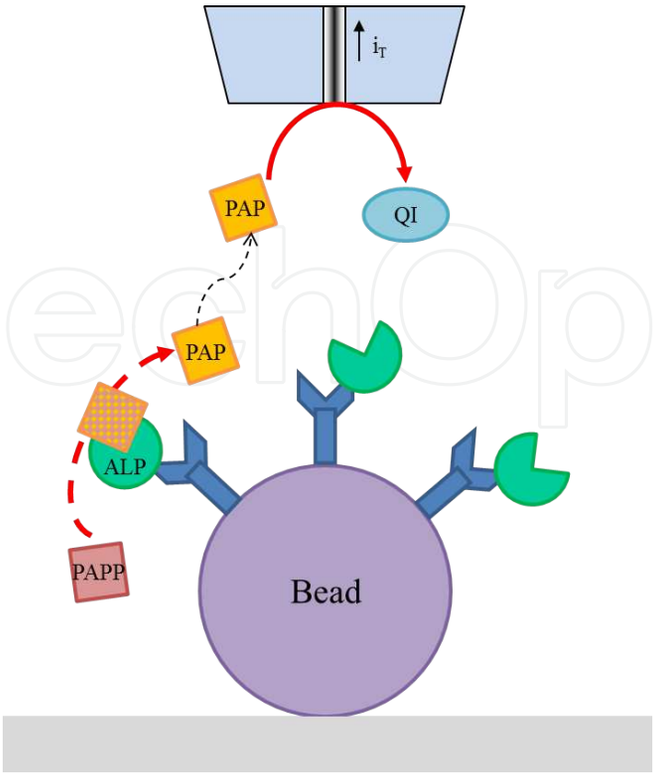

Figure 5. The principle of detection with magnetic beads combined with enzyme reaction. The surface of the bead is coated with primary antibody that has accessible Fab groups responsible for binding the analyte. The label alkaline phosphatase (ALP) is attached to the captured analyte as a conjugate with the second Ab. The ALP catalyses the conversion of redox inactive 4-aminophenyl phosphate (PAPP) in solution to the redox active *p*-aminophenol (PAP) not presented in the bulk of the solution. The faradaic current at the tip, i_T, is caused by the oxidation of PAP to the quinone imine (QI). A quasi-stationary and hemispherical diffusion of PAP can be expected over the beads.

2.3. Quantum dots

Other kinds of NPs widely used as labels for determination of proteins and DNA are semiconductor nanocrystals, quantum dots (QDs). Efficient methods for the preparation of quantum dots and their functionalization with biomaterials have been recently developed [45]. These nanoparticles are applied for labelling of biomaterials in biorecognition processes (e.g., DNA sensing) [46]. In generally, the QDs are employed as an electro sensitive label and detected by various voltammetry techniques, almost by differential pulse voltammetry [8]. Connection of QDs with SECM method is very outstanding. However, several works are presented in this area of research as follows. Morphological analysis of PbSe was shown by *Zimin, S., et al.* [47]. They investigated the morphology of the surface of PbSe/CaF2/Si(111) epitaxial structures after anodic electrochemical etching. Two possible morphological types of PbSe nanostructured surficial porous layers were distinguished. Agglomerated nanoislands with 80-400 nm lateral sizes and 70 nm average separating gaps were observed for the anodized films with initial flat terraced surface. *Liu, G. J.* group [48] presents the investigation of semiconductor photocatalyst - quaternary-alloyed Zn*x*Cd1-*x*S*y*Se1-*y*, by SECM. The photoelectrochemical properties were evaluated by scanning electrochemical microscopy in the photoelectrochemical mode using an optical fibre tip attached to a Xe lamp as an excitation

source. The spot with a precursor composition Zn 0.3 Cd 0.7 S 0.8 Se 0.2 (elemental ratio, 1:2.12:1.75:0.81) showed the highest photocurrent under 150 W Xe lamp irradiation.

It is obvious from the above mentioned application that connection of QDs with SECM is very unusual and disparity in application point of view. This research area forms the big unexplored and perspective potential for the further investigation.

2.4. Gold nanoparticles

Creation of the small specific modified area on the gold surface is possible due to modification of the gold nanoparticles instead of the modification of the whole surface of the substrate electrode. This way can offer specific modification in the small dimensions. The other important reason for the application of nanoparticles lies in the fact that, whilst the bulk material is incredibly inert, nanostructured gold can exhibit exceptional catalytic activity [49].

Application of gold nanoparticles is obviously affected by many conditions. The most important are the size and the shape of the particles. The size effect has been clearly presented by *Wain, A. J.* [50]. In this work the influence of particle size on the electrocatalytic behaviour of commercially available spherical gold nanoparticles (AuNPs) is demonstrated. The experiment focused on the oxygen reduction reaction (ORR) and the electrooxidation of hydrogen peroxide using redox competition and tip collection modes. For both reactions studied the electrocatalytic activity, normalized to surface area, was observed the increase with decreasing particle diameter in the range 5-50 nm. It is necessary to connect this result with the role of mass transport on the observed particle size effects. A 50 nm AuNP has a surface area 100 times greater than a 5 nm AuNP. Therefore, for a fixed surface area, a spot consisting of 50 nm AuNP has a factor of 100 fewer particles than a spot consisting of 5 nm AuNPs. However, under conditions of convergent diffusion, the mass transport limited flux to a 50 nm particle is ten times greater than to a 5 nm particle. Taking these two factors into account, the total flux to a spot of 5 nm particles is expected to be ten times greater than to a spot of 50 nm particles which, under mass transport limited conditions, could lead to an enhancement in the apparent electrocatalytic activity.

Influence of the shape of the gold particles was investigated by *Sanchez-Sanchez, C. M. et al.* [51]. The authors used three types of nanoparticles: semi-spherical particles with a particle size of 3.1±0.46 nm, cubic shaped (≈ 85%) particles in dimension 43.8±1.1 nm and short nanorods with an average width of 10.9±1.2 nm and length of 42.9±5.3 nm. The influence of the nanoparticle shape was investigated through the electrocatalytic activity for the ORR. The results demonstrate that cubic gold NPs are the most active towards ORR in 0.1M NaOH, followed by the spherical gold NPs and, finally, by the short gold nanorods.

The same authors investigated the influence of platinum nanoparticles on the ORR [52]. They employed TG/SC mode to study ORR on shape-controlled Pt nanoparticles. The catalytic activities of four types of Pt nanoparticles, spherical, cubic, hexagonal, and tetrahedral/octahedral, were compared. Hexagonal particles exhibited the highest activity towards ORR in acid electrolytes.

As it is presented above, the influence of the size and shape was investigated through the electrocatalytic measurements - the aqueous phase oxygen reduction reaction (ORR). The ORR

http://dx.doi.org/10.5772/57203

on gold can take place via a 2-electron pathway yielding hydrogen peroxide or a 4-electron route generating water. The reaction mechanism and kinetics are known to be structure sensitive. On Au(1 0 0) single crystal surfaces the 4-electron mechanism dominates, on Au(1 1 1) and Au(1 1 0) the 2-electron mechanism is more significant. The activity of these facets is known to decrease in the order Au(1 0 0) > Au(1 1 0) > Au(1 1 1) [53, 54]. Therefore by changing the relative proportions of these low index planes present on the surface of AuNPs one can essentially tune their ORR electrocatalytic activity [50, 55]. This is in agreement with above-mentioned experiment comparing various types of nanoparticle shape. It has been concluded that the highest activity is for the cubic structure where the faces of the cube is oriented along the (1 0 0) direction, in all cases, which is in agreement with the theoretical symmetry expected for a cube.

The very good example of the SECM study of gold nanoparticles (and theirs modification) was presented by *Huang et al.* [56]. They show the combination of AFM and SECM methods for the detection of individual ~20 nm sized gold nanoparticles. The scheme is shown in Fig. 6. The physical and electrochemical properties of functionalized particles by redox-label PEG chains were studied. The redox PEGylated nanoparticles were assembled onto a gold electrode surface, forming a random nanoarray, and interrogated *in situ* by a combined AFM-SECM nanoelectrode probe. In so-called mediatortethered (Mt) mode, AFM-SECM affords the nanometer resolution required for resolving the position of individual nanoparticles and measuring their size, while simultaneously electrochemically directly contacting the redox-PEG chains they bear.

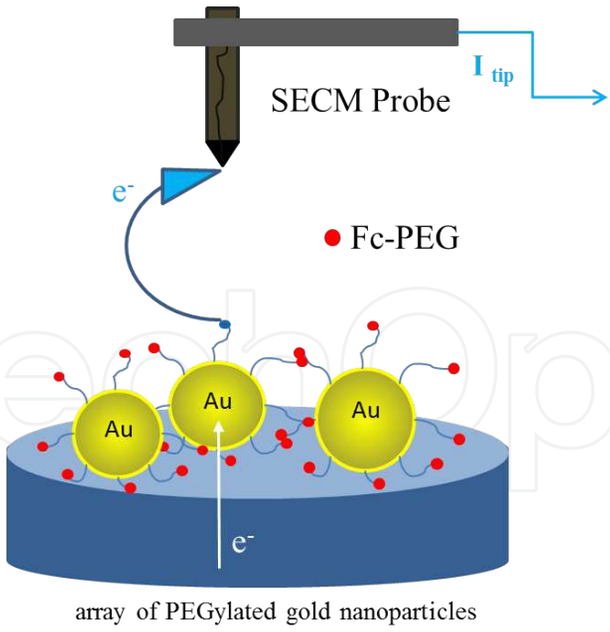

Figure 6. Combination of atomic force and electrochemical scanning microscopy (AFM-SECM) is presented as an analytical tool for simultaneous study of the physical and electrochemical properties of individual ≈ 20 nm sized gold nanoparticles functionalized by redox-labelled PEG chains. The measurements were done in a 0.1 M pH 6 citrate buffer solution. The tip was biased at a potential of E_{tip} = +0.3 V/SCE, while a potential of E_{sub} = -0.1 V/SCE was applied to the substrate.

The nanoparticle acts both as a scaffold and as a nano-electrode, mediating electron transfer between the underlying gold substrate and the redox labels of the PEG. The AFM-SECM probe is brought in "molecular" contact with the macromolecular PEG layer covering the nanoparticle. The tip and substrate are biased so that the redox label is alternatively oxidized at the tip and re-reduced at the substrate. The tip was biased at a potential of E_{tip} = +0.3 V/SCE, while a potential of E_{sub} = -0.1 V/SCE was applied to the substrate in 0.1 M citrate buffer. This redox cycling generates a specific tip electrochemical current whose intensity depends on the (time-averaged) tip-substrate distance, the Brownian dynamics of the PEG, and the local surface concentration in PEG [56]. The use of tapping mode allows the tip-substrate distance to be fixed so that the tip current specifically probes the presence of the labelled molecule and its surface concentration (coverage) on the nanoparticle. The dual measurement of the size and current response of single nanoparticles uniquely allows the statistical distribution in grafting density of PEG on the nanoparticles that was determined and correlated to the nanoparticle diameter.

3. Electrochemical imaging

3.1. Characterizing of molecules and their interactions

Scanning electrochemical microscopy is the useful tool for the investigation of the electro-behaviour of micro and nano objects. The wide range of applications is possible; for the simplicity, it is divided into several fields of research as follows: characterization of entities, measurement of charge and mass transport, biochemical processes, reaction kinetics, energy measurement, and degradation processes [2, 4, 12]. Each presented direction of the research can be further divided into the subunits. The first mentioned area, characterization of entities, could be divided in point of view of the material background, size of detected objects, physicochemical properties, reactivity etc. Interaction phenomenon is closely connected with characterization of entities, on which participates almost at least one biocompound (oligonucleotide, protein, enzyme, antibodies, lipids or the whole cell).

3.1.1. DNA

The first SECM images of DNA were reported by *Guckerberger et al.* in 1994. Since this point much progress has been made and the advance to the development of the fabrication techniques of DNA microarrays has been achieved. The detection of various base pairs is critical for the study, diagnosis and treatment of genetic diseases [6].

The simplest form of nucleic acid detection was described by *Wang et al.* who exploited the intrinsic electrochemical properties of the guanine residue in the DNA duplex [57]. Surface-immobilized DNA molecules were detected by the generation/collection mode of SECM through the oxidation of guanine residues by tip generated Ru complex. The second approach to imaging DNA and the hybridisation event is to use electrochemically active labels. *Wang et al.* [58] reported application of the silver nanoparticles in combination with SECM to image a DNA microarray. Silver nanoparticles were deposited at sites where hybridisation had

http://dx.doi.org/10.5772/57203

occurred. The result was an area over which positive feedback could occur as a consequence of mediator recycling (site of silver deposition).

The development of reagentless procedures, by which DNA hybridisation could be detected, was presented by *Turcu et al.* [59, 60]. They detected the hybridisation process through coulomb interactions between the negatively charged sugar phosphate back bone of the immobilised oligonucleotide and the $[Fe(CN)_6]^{3-}$ as a free diffusing redox mediator.

Hybridisation process of DNA was investigated by *Roberts et al*. too [6]. They studied adsorption of genomic DNA and subsequent interactions between adsorbed and solvated DNA. They prepared microarray of polyethylenimine (PEI) film deposited on a screen-printed carbon substrate using the SECM. There was single stranded DNA electrostatically adsorbed on the surface of the polyethylenimine. The further adsorption of complementary single stranded DNA on the surface was observed [6].

3.1.2. Proteins

The SECM protein detection was widely investigated especially by *Girault* group [61-64]. They used a detection system based on the tagging adsorbed proteins with silver nanoparticles (Fig. 7). A positive feedback was obtained when a platinum tip approached the silver-tagged proteins in a 1mM $[Os(bpy)_3]^{2+}$ aqueous solution. The feedback loop was created by $[Os(bpy)_3]^{3+}$ generated by the tip, diffused toward the silver-tagged proteins and next reduced back to $[Os(bpy)_3]^{2+}$. Compound $[Os(bpy)_3]^{2+}$ was chosen as a mediator because the standard redox potential for the couple $[Os(bpy)_3]^{3+/2+}$ (0.631 V vs SCE) is positive enough so that its oxidized form is able to accept an electron from Ag atoms attached to the protein on the substrate (Ag^+/Ag standard potential is 0.558 V vs SCE). Furthermore, this potential is not too close to the positive limit of the potential window in water.

Another *Girault*s work [64] presents the protein detection based on the tagging of free cysteines and other nucleophiles in proteins and peptides by benzoquinone. The tagged proteins are detected by the mediated reduction of benzoquinone with a redox species ($K_3[Fe(CN)_6]$ or $K_3[IrCl_6]$) produced electrochemically at the SECM tip. In addition, the SECM investigation of adsorption and binding of protein to the polymer surface was done by *Glidle et al*. [65]. This phenomenon was studied according to the application of proteins to the biosensor platform.

3.1.3. Enzymes

The recent SECM studies of immobilized enzymes focus on two areas: measuring the catalytic enzyme activity and micropatterning the surface with enzymes [2]. Two SECM-based approaches, generation/collection and feedback mode, are applied to the redox enzymes detection. The GC mode is more sensitive and can be employed when enzyme kinetics are too slow for feedback measurements. Opposite this, the feedback mode is more suitable for enzymes with high activity [12].

Both directions of the enzyme research by SECM are covered by the work of *Wittstocks* group [43, 66-70]. The first case is represented by the experiment in which the direct mode of SECM was used for the local deposition of oligonucleotide patterns on thin gold films and the GC

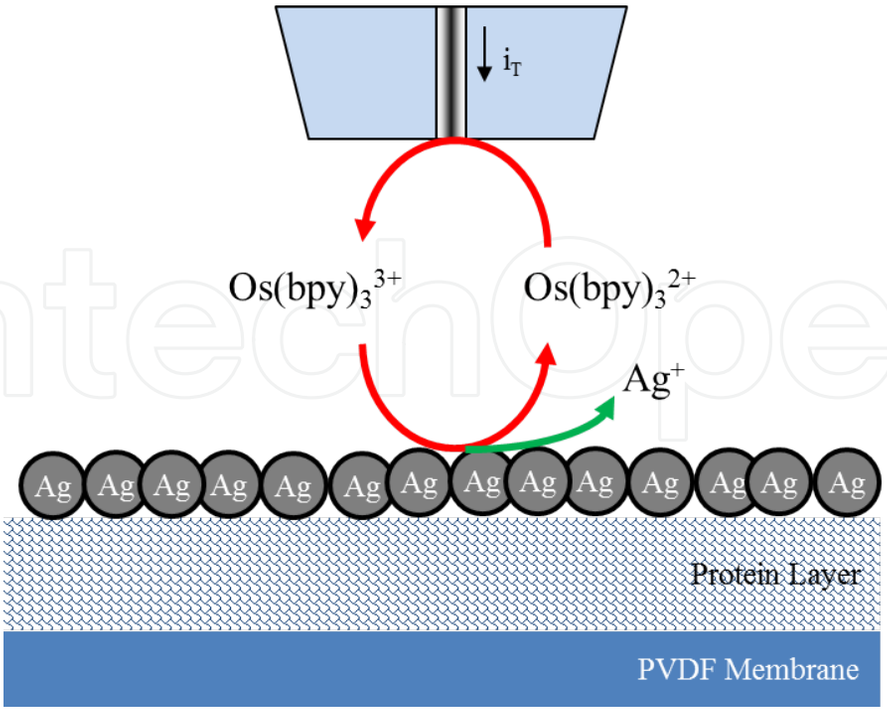

Figure 7. Schematic representation of the electrochemical principle used for protein detection through silver nanoparticles. The working electrode is held at +0.7 V vs Ag/AgCl; at this value the oxidation of the redox mediator is observed. When the tip is close enough to the sample, the oxidized form of the mediator reacts with the silver nanoparticles leading to the production of Ag^+. 1 mM $[Os(bpy)_3]^{2+}$ aqueous solution as a mediator and 0.1 M KNO_3 as a supporting electrolyte were used.

mode was applied for the determination of the amount of surface-accessible oligonucleotides [66]. This process was monitored through the specific system created by biotin-labelled complementary strand connected with streptavidin and biotin-labelled β-galactosidase. The activity of the linked β-galactosidase was mapped with SECM in the GC mode by monitoring the oxidation of *p*-aminophenol (PAP) created in the enzyme-catalysed hydrolysis of *p*-aminophenyl-β-d-galactopyranoside. Micropattering of the surface with enzymes is presented in another *Wittstock*s work [67] where the monitoring of patterned enzyme layers containing glucose oxidase and horseradish peroxidase was described. These layers were created by a combination of microcontact printing (MCP) and local electrochemical desorption followed by chemisorption of functionalized thiols or disulphides. The reactions of two enzymes, horseradish peroxidase (HRP) and glucose oxidase (GOx), were studied.

In the last year one interesting work related to enzyme systems was published [71]. This work is focused on the study of multi enzyme systems by SECM. There is presented study of the kinetics of a two-enzyme coupled reaction, specifically acetylcholine esterase and choline oxidase. This type of experiment push the boundaries further because of approach to the real systems. The biological metabolism process is obviously given via a group of enzymes working together in sequential pathways. The exploration of the metabolism mechanism requires the understanding of the multi-enzyme coupled catalysis systems.

http://dx.doi.org/10.5772/57203

3.1.4. Antibodies

The most of SECM interaction experiments is limited through the fact that one of reaction compound is bound with (onto) the surface (glass, gold electrode, carbon electrode) [72]. The specificity of the antibodies binding allows performing label-free experiments. This trend is obvious in the last three years, where some works related to this phenomenon have appeared. *Le et al.* [73] presents label-free immunosensor based on a biotinylated single-chain variable fragment antibody immobilized on co-polypyrrole film. Immunosensor device formed by immobilization of a biotinylated single-chain antibody on an electropolymerized copolymer film of polypyrrole using biotin/streptavidin system was demonstrated for the first time. The response of the biosensor toward antigen detection was monitored by electrochemical analysis of the polypyrrole response by DPV, not by SECM. The SECM system monitoring the interrogation of antibody–antigen interactions was presented by *Holmes et al.* [74, 75]. Screen-printed carbon electrodes were used as a substrate for the deposition of a dotted array, where the dots consisted of biotinylated polyethyleneimine. These were then further derived, first with neutravidin and then with a biotinylated antibody to the protein neuron specific enolase (NSE). In the next experiments biotinylated antibody towards a relevant antigen of interest (PSA, NTx, ciprofloxacin) were used. These antigens were chosen for their clinical relevance but also since, they display a broad range of molecular weights to determine the influence of the size of the antigen. SECM using a ferrocene carboxylic acid mediator showed clear differences between the array and the surrounding unmodified carbon. Binding of the antigen was accompanied by a measured increase in current response, which may be explained in terms of protein electrostatic interactions and hydrophobic interactions to the mediator. Control experiments with other proteins showed only a non-specific binding across the whole of the substrate, thereby confirming that specific binding occurs between the antibody and antigen on the surface of the dots.

3.1.5. Lipids

The application of lipids by SECM is focused on the characterization of lipid mono and bilayers, especially on the charge transfer through lipid membranes [9, 17, 76]. The research in this area could be divided in three main streams.

The first case is about applying of SECM technique for investigation of membrane transport, mainly through the pores [77, 78]. *Wilburn et al*. [79] presents the utilisation of SECM for the creation of voltage-gated biological ion channels. These were simulated by insertion of the peptaibol antibiotic alamethicin into reconstituted phosphatidylcholine bilayer lipid membranes (BLMs). SECM was utilized to probe initial BLM resistivity, the insertion of alamethicin pores, and mass transport across the membrane.

Membrane transport of redox species through the membrane, this time without pores or channels, is the second direction. *Zhan and Bard* [80] present experiment based on the immobilisation of liposome structure (15-50 μm in diameter) filled with the Ru(2,2′-bipyridine)$_3^{2+}$ as a redox mediator on the glass substrates (Fig. 8). Conical carbon fibre tips of submicrometer size were used to approach, image, and puncture. This way the leakage of redox mediator through the lipid membrane was probed. The last direction of research is focused to the charge/

electron transfer through the lipid layers. Out of the study of the basic charge transfer processes [81-83], there were studied the absorption procedures as metal ion absorption [84] so as drug absorption [85].

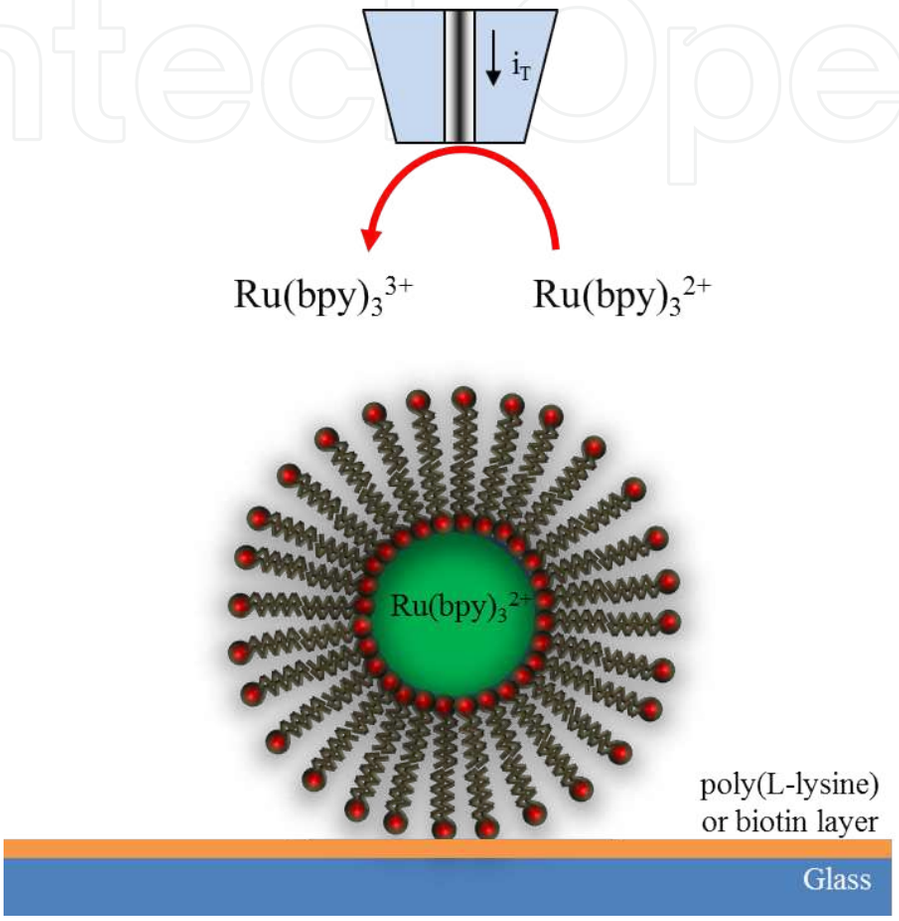

Figure 8. Liposomes of 15-50 nm were immobilized on glass substrates via either poly(L-lysine) or biotin-avidin-biotin sandwich structure; these liposomes were probed by a submicrometer-sized carbon fibre tip controlled by the SECM. The immobilized liposomes were imaged by SECM in a solution of 1.0 mM ruthenium^{3+} hexamine in 100 mM phosphate buffer, pH 7.0. The leakage of $Ru(bpy)_3^{2+}$ from individual liposomes was detected by placing a tip near the liposome and monitoring the current for $Ru(bpy)_3^{2+}$ oxidation.

3.1.6. Cells

The issue of cell studying by SECM is so wide and varied that the short overview is not possible. There are various imaging ways of an individual cell based not only on its surface topography, but also on cellular activities such as photosynthesis, respiration, electron transfer, single vesicular exocytosis, and membrane transport. Therefore the two best reviews in this field are cited [9, 86].

http://dx.doi.org/10.5772/57203

3.2. Various current levels — Images of modification

Modification of surfaces is the introduction of well-defined, directly local changes in the chemical or physical properties of such surfaces. This includes etching processes, deposition of materials, and chemical modification of the surface material. As a scanning probe technique, SECM is predestined to generate chemical changes locally. Instead of detection, the SECM can serve as the preparation tool for microstructures creation. In general, two main ways of application are reported, the direct mode and the feedback mode [2]. The usage of direct mode is based on the fact that the tip is held in a close proximity to the substrate, and the voltage is applied between them to cause the desired reaction at the substrate. In the feedback mode surface patterning, a redox mediator is present in the solution. The tip-generated redox species must be able to induce the desired reaction (i.e., deposition or etching) at the substrate and be regenerated on its surface. The benefit of the feedback mode deposition is that the substrate needs not be a conductor [2]. This phenomenon was described very well in a review of *Sun et al.* [2], where the authors presented works up to year 2007, let us focus the next text on the applications presented just since the year 2007 till now.

The surface modifications are still focused on the enzyme applications. *Li et al.* prepared nanometer-sized carbon fibre disk electrode and applied them to micropattern active horseradish peroxidase (HRP) coupled with a carbon fibre disk electrode as the SECM tip. Active HRP substrates were fabricated on the substrates coated with streptavidin by binding biotinylated HRP. In one work [87] for the deactivation of other regions on the HRP micropatterns the authors used the reactive species generated on the electrode as the tip of SECM held at 1.7 V through oxidation of Br^- in 0.20 M phosphate buffer (PB) containing 2.5 x 10^{-2} M KBr and 2.0 x 10^{-3} M BQ (pH 7.0). The micropatterns of active HRP were characterized using the feedback mode of SECM in PB containing 2.0 x 10^{-3} M BQ and 2.0 x 10^{-3} M when the tip potential was held at -0.2 V. Another work from *Li et al.* [87] presents deactivation of other region of the HRP micropatterns by OH- generated at the tip held at -1.7 V in 1.0 M KCl containing 2.0 x 10^{-3} M benzoquinone (BQ) (pH 8.0). The feedback mode of SECM with a tip potential of - 0.2 V was used for characterizing the active HRP micropatterns in 1.0 M KCl containing 2.0 x 10^{-3} M BQ and 2.0 x 10^{-3} M H_2O_2.

Another application of HRP in patterning experiments has been described by *Roberts et al.* [88]. In this case the immobilisation in a patterned fashion onto glass slides is presented. Microarray of HRP islands was deposited on amino-modified glass slides using glutaraldehyde cross-linking combined with the SECM and this was used as a micro-deposition device [88].

Application of nitrogen compounds were shown as a good tool for the patterning technique by SECM. *Cougnon et al.* [89] showed production of diazonium salts from nitro compounds. The nitro precursor is reduced at the tip to the amine, which is diazotized in the interelectrode space. The tip acts as a source of diazonium salts, allowing sample derivatization just under the tip. Extension of this work has been published in another Cougnons work [90] where the authors present the second mechanism of microstructuring. This time the process starts with the reduction of a nitro-containing compound at the scanning electrochemical microscope tip. After diffusion in the interelectrode gap, the amine is oxidized on a gold surface, thus resulting in a local derivatization. *Janin et al.* [91] describes another way of pattering based on the

electrochemical grafting of nitrophenyl groups onto platinum ultramicroelectrode (UME). The grafting was made using the electrochemical reduction of nitrophenyldiazonium and the possibility to reduction the diazonium onto Pt UME was observed. Extension of the above-mentioned procedure by creating of a *p*-nitrothiophenol SAM was described by *Schwamborn et al.* [92]. The reduction of the terminating nitro groups of a *p*-nitrothiophenol SAM under formation of hydroxylamine or amino groups is invoked using the direct mode of SECM. The local modification of the redox states was visualized by using the feedback mode of SECM. The current at the Pt tip electrode is determined by the electron-transfer rate for re-oxidation of the redox mediator on the sample surface. Selective post-functionalization with an avidin-alkaline phosphatase conjugate allows visualization of the microstructure using the generator-collector mode of SECM too. Simplification of the surface modification by grafting procedure on the gold substrate by 4-azidobenzenediazonium with SECM was presented by *Coates et al.* [93]. The electrografted spots of diazonium were in this case performed by positioning a SECM platinum tip at a given distance above the gold substrate and the SECM was used in a three-electrode configuration (the Pt tip serving as a microanode). As the mediator acetonitrile containing 5 mM 4-azidobenzenediazonium and 0.1 M Bu_4NBF_4 was used.

Usage of various nanoparticles or nano structured materials expands through the wide range of applications and techniques. SECM is no exception. Preparation of some nanoparticles was described in literature in recent few years. Preparation of gold nanoparticles is described by many authors [94], and possibility of SECM application for preparation of gold nanostructures exists. Process of local electrodeposition of gold nanoobjects, namely gold nanorods, is described in work of *Fedorov* and *Mandler* [95]. In this process a gold microelectrode was the source of the gold ions whereby double pulse chronoamperometry was employed to generate initially Au seeds, which were further grown under controlled conditions.

The silver nanoparticles were prepared either at liquid interface [96] or on the SAM monolayer [97]. The creation at the liquid interface is based on the electron transfer reaction between aqueous Ag^+ ions generated by anodic dissolution of an Ag disk UME, and bis(pentamethyl-cyclopentadienyl) iron (decamethylferrocene, DMFc) in a 1,2-dichloroethane (DCE) phase [96]. The second way, usage of SAM monolayer, is based on the local deposition of Ag nanoparticles (NPs) on ω-mercaptoalkanoic acid SAMs. SECM was used for generating a controlled flux of silver ions by anodic dissolution of silver microelectrode close to the SAMs modified Au(1 1 1) surface [97].

3.3. Quantification of electrochemical images

SECM is a powerful tool for studying structures and processes in micro and submicro meter-sized systems. It can probe electron, ion, and molecule transfers as well as other reactions at solid-liquid, liquid–liquid, and liquid-air interfaces. With the same setup, several SECM modes of operation can be realized, see section 1.2. The most widespread is the feedback mode, tip generation/substrate collection (TG/SC) mode and the substrate generation/tip collection (SG/TC) mode.

The quantitative SECM theory has been developed for various heterogeneous and homogeneous processes and different tip and substrate geometries. In general, theoretical SECM

http://dx.doi.org/10.5772/57203

dependencies can be generated by numerically solving partial differential equations. In some cases, analytical approximations allow for easier generation of theoretical dependencies and analysis of experimental data. The most quantitative studies were carried out under steady-state conditions, because the non-steady-state SECM response depends on too many parameters that allow any possible presentation set of working data. The steady-state theory is simpler and often can be expressed in the form of dimensionless working curves or analytical approximations.

For the understanding of mathematical description of the SECM experiments, it is necessary to present some general characteristic and notations. The first assumption, which is generally accounted, is the fact that experiments are made with a redox mediator in a solution where only its diffusion is important (migration and convection are neglected). Its bulk concentration is written as c and D is used for its diffusion coefficient (same value assumed for red or ox form in most of the cases). The tip electrode is generally a disk shaped microelectrode where is characterised the radius of the conductive core, a; and the total tip radius, r_g. The dimensionless parameter RG is defined as follows: $RG = r_g/a$ and is normally ≤ 10. The tip placed at a distance d from the substrate, the dimensionless parameter L is defined as d/a). The potential of the tip is almost always set to a value where the redox reaction of the mediator is rapid and reversible: only mass transport defines the current value. The absolute value of the current going through the tip electrode (respectively through the substrate) is usually written as i_T (respectively i_S). Normalized current is commonly used in SECM experimental reports, defined by the comparison with the tip current when the tip is very far from the studied substrate: $i_T/i_{T\infty}$. Finally the positive feedback situation is referred with the "con" subscript (tip above a conductive substrate) and the negative one with "ins" subscript (tip above an insulating substrate).

The simplest situation in SEMC measurements is the steady state feedback mode, when the tip is immersed in a solution containing a redox mediator (an oxidizable species R) [2]. By applying the positive potential to the tip, the oxidation of R occurs

$$R - ne^- \longrightarrow O \tag{4}$$

at a rate governed by diffusion of R to the UME surface. If the tip is far (greater than several tip diameters) from the substrate the steady-state current, $i_{T\infty}$ is given as follows

$$i_{T\infty} = 4nFDca \tag{5}$$

where F is the Faraday constant, n is the number of electrons transferred in reaction, D and c are the diffusion coefficient and the bulk concentration of R and a is the tip radius.

When the tip is brought to within a few tip radii of a conductive substrate surface, the O species formed in the reaction (Eq. 4) diffuses to the substrate where it can be reduced back to R

$$O + ne^- \longrightarrow R \tag{6}$$

This process produces an additional flux of R to the tip and hence ''positive feedback'', the increase in tip current ($i_T > i_{T\infty}$). With shorter the tip-substrate separation distance (d), the tip current is larger. When reaction (Eq. 6) is rapid, than $i_T \rightarrow \infty$ as $d \rightarrow 0$.

If the substrate is an inert electrical insulator, the tip generated species, O, cannot react at its surface. At small d, $i_T < i_{T\infty}$, because the insulator blocks the diffusion of species R to the tip surface (''negative feedback''). The closer the tip to the insulator substrate, the smaller the i_T, with $i_T \rightarrow 0$ as $d \rightarrow 0$.

The specification that has to be underlined in the context of SECM is that this exact analytical expression is valid only for an infinite RG value: Application of microelectrode with finite RG value led to the modification of equation 1 as follows:

$$i_{T\infty} = 4nFDca\beta(RG) \tag{7}$$

Various approximate expressions of β(RG) can be found in the literature and the better expressions are as follows:

$$\beta = 1 + \frac{0.1380}{(RG - 0.6723)^{0.8686}} \tag{8}$$

$$\beta = 1 + 0.639\left(1 - \frac{2}{\pi} ArcCos\frac{1}{RG}\right) - 0.186\left[1 - \left(\frac{2}{\pi} ArcCos\frac{1}{RG}\right)^2\right] \tag{9}$$

3.3.1. Homogeneous reaction in solution

The first theoretical study of SECM feedback for homogeneous reactions in solution published in 1994 [98] showed that there is a linear relationship between the current measured through the tip, i_T, and the current going through the substrate, i_S. This relationship can be rewritten as follows:

$$i_T = i_S\left(1 - \frac{i_T^{ins}}{i_T^{con}}\right) + i_T^{ins} \tag{10}$$

i_T^{ins} and i_T^{con} being the negative and positive feedback currents that would been obtained in the same geometric configuration (same L). It is necessary to kept in mind that this equation describes the reaction in an electrolyte. As soon as no homogeneous reaction occurs on the substrate or tip (with connection vice versa), the relationship between the tip and substrate steady-state current is very easy [99]:

$$i_T = i_S = i_T^{con} \tag{11}$$

http://dx.doi.org/10.5772/57203

3.3.2. Heterogeneous reaction

Study of heterogeneous reaction, exactly heterogeneous electron transfer, is widely used application in SECM determinations. The kinetics of heterogeneous electron transfer can be determined with high lateral resolution while scanning a tip parallel to the surface. Distance-dependent measurements provide quantitative information on sample properties.

One step heterogeneous electron transfer reaction is the simplest case of these types of reactions. An analytical approximation which is often used is valid for RG = 10 and normalized distances $0.1 \le L \le 1.5$. The current-distance curves for an irreversible heterogeneous reaction occurring at the substrate while the tip process is diffusion-controlled can be calculated from

$$I_T(L) = \frac{i_T}{i_{T\infty}} = I_S(L)\left(1 - \frac{I_T^{ins}(L)}{I_T^{con}(L)}\right) + I_T^{ins}(L) \tag{12}$$

$$I_S = \frac{0.78377}{L\ (1 + 1/\Lambda)} + \frac{0.68 + 0.3315exp(-1.0672/L)}{1 + F(L, \Lambda)} \tag{13}$$

where I_T^{ins} and I_T^{con} are normalized current related to the insulating substrate, and diffusion-controlled regeneration of redox mediator, respectively. The analytical approximations for these two values are [3]:

$$I_T^{con}(L) = \frac{0.78377}{L} + 0.3315exp\left(\frac{-1.0672}{L}\right) + 0.68 \tag{14}$$

$$I_T^{ins}(L) = \frac{1}{0.15 + \frac{1.5385}{L} + 0.58exp(-1.14/L) + 0.0908exp\left[(L - 6.3)/1.017L\right]} \tag{15}$$

In this place it is important to highlight that the value of I_T^{ins} depends on the RG value too [100]. For the various RG value were calculated the parameters of this equation and these are able to read in [2].

Back to the Eq. 12 where it is necessary to define the remaining variables. I_s is the kinetically controlled substrate current. Λ is defined as $\Lambda = k_f d / D$, where k_f is the heterogeneous rate constant, and D is the diffusion coefficient. The function F depends on the L and Λ, is defined as follows: $F(L, \Lambda) = \left(\frac{11}{\Lambda} + 7.3\right) / (110 - 40L)$.

Notwithstanding above presented equations (Eq. 12 and 13) were derived for one step heterogeneous electron transfer reactions, it has been proofed that are applicable to more complicated substrate kinetics (e.g., liquid–liquid interfacial charge transfer, ET through self-assembled monolayers and mediated ET in living cells [2]).

On the other hand, study of the heterogeneous electron transfer reactions at SECM is possible to view from the opposite. For the finite heterogeneous kinetics at the tip and diffusion-controlled mediator regeneration at the substrate, an approximate was recently obtained for I_T as a function of tip potential E, and L [101]:

$$I_T(E,\ L\ ) = \frac{0.78377}{L\ (\theta + 1/\kappa)} + \frac{0.68 + 0.3315exp(-1.0672/L\ )}{\theta\left[1 + \frac{\pi}{\kappa\theta}\frac{2\kappa\theta + 3\pi}{4\kappa\theta + 3\pi^2}\right]} \tag{16}$$

where

$$\kappa = \pi\lambda exp\left[-\alpha F\left(E - E^{o'}\right)/RT\right]/\left(4I_T^{con}\right) \tag{17}$$

$$\theta = 1 + exp\left[F\left(E - E^{o'}\right)/RT\right]D_o/D_R$$

$$\lambda = k^o a/D$$

$E^{o'}$ is the formal potential, α is the transfer coefficient, $I_T^{con}(L\ )$ is the normalized tip current for the same L the diffusion-controlled positive feedback at a conductive substrate, as defined by Eq. 14.

3.3.3. GC mode

The above-presented approximation models are related to the feedback mode of SECM determinations. The application of GC mode is connected with some difficulties in the quantitative interpretation of the measured results [17]:

- if the active region of the sample is to large, no steady-state situation is established. The local concentration depends not only on the position of the UME but also on the time that has passed since the onset of the reaction.
- the moving of probe disturbs the macroscopic diffusion layer of the sample through convection. This effect hinders the diffusion of reagents to the sample region underneath the UME.
- an enhancement of the current according to the principle of positive feedback can reach significant values if $d < 3a$.

Minimization of the quantitative issues is possible due to working with as small as possible UMEs (small RG). In these cases, the disturbance of the sample diffusion layer is minimized and feedback effects can also be neglected at small values of d. The lateral resolution is always poorer in GC mode than in the corresponding feedback experiments [17]. However, the GC mode offers a much higher sensitivity than feedback mode because the flux of reagents coming from the sample is measured essentially without a background signal [102]. This makes the GC mode appropriate for the investigation of immobilized enzymes and cells.

3.3.4. Numerical models

The analytical approximations presented above are best fits to numerical simulations of the diffusion problems for relatively simple and well defined electrochemical systems, e.g., an inlaid disk electrode approaching a flat, infinite, and uniformly reactive substrate surface. In most quantitative SECM experiments, the use of such approximations could be justified.

http://dx.doi.org/10.5772/57203

However, no analytical approximations are available for more complicated processes and system geometries, and so one has to resort to computer simulations.

The above mentioned models suggested the disk shaped tips. In real experiments, it is difficult to assume the ideal disk shaped tip. Production of tips, which may be similar to ideal model, is very difficult, especially when they have to be nanometer-sized. Characterization of the non-disk shaped tips (sphere cups, spheres, rings, ring disks and etched electrodes), experimental approach curves were obtained and then compared to simulated ones [3].

The solution of the diffusion phenomenon has been developed mostly as two-dimensional axi-symmetric diffusions. Even for an idealized situation (i.e. a flat, planar substrate, strictly perpendicular to the axis of the well-shaped disk tip) only numerical solutions can be obtained. The most important step is the validation of calculated data relate to the real measurements. Similar questions arise when the topography of substrate is complicated and/or its surface reactivity is highly non-uniform.

The most popular method for mathematical calculations of diffusion effect by SECM has been presented for the first time by *Fulian et al*. [13, 14]. They introduced the boundary element method (BEM), which is more suitable for problems with regions of complex or rapidly changing geometries. They used BEM to simulate the current responses for different SECM situations, such as a non-disk tip approaching a flat substrate; a flat disk tip over a hemispherical or a spherical cap-shaped substrate or a tilted substrate; a lateral scan of a flat disk tip over an insulating/conductive boundary. The next improvement and extension of this method, mostly related to the specific experiment simulation, has been published by many authors [103-105].

4. Conclusions

The SECM is the widely used technique in material and process investigation. Especially effects connected with electron transfer are studied. Micro and nano sized tips used in these experiments allow to measure nano and sub-nano currents levels and this way allow to describe the very small particles / surfaces. Significant progress has been made over the last five years in both quantitative (e.g. kinetic experiments) and qualitative (e.g. topographic imaging) applications of SECM to studies of structures and processes on the nanoscale. Combination of nanoparticles and SECM shifts the possible usage of this technique to the new horizon. This chapter summarizes the basic knowledge in the field of SECM in relation to study of nanoscale systems, specifically nanoparticles.

Acknowledgements

Financial support from the following projects NanoBioMetalNet CZ.1.07/2.4.00/31.0023 and NanoBioTECell GA CR P102/11/1068 is highly acknowledged.

Author details

David Hynek[1,2], Michal Zurek[1,2], Petr Babula[1], Vojtech Adam[1,2] and Rene Kizek[1,2*]

*Address all correspondence to:

1 Central European Institute of Technology, Brno University of Technology, Brno, Czech Republic

2 Department of Chemistry and Biochemistry, Faculty of Agronomy, Mendel University in Brno, Brno, Czech Republic

References

[1] Bard AJ, Denuault G, Lee C, Mandler D, Wipf DO. Scanning electrochemical microscopy - A new technique for the characterization and modification of surfaces. Accounts Chem Res. 1990 Nov;23(11):357-63.

[2] Sun P, Laforge FO, Mirkin MV. Scanning electrochemical microscopy in the 21st century. Phys Chem Chem Phys. 2007;9(7):802-23.

[3] Mirkin MV, Fan FRF, Bard AJ. Scanning electrochemical microscopy. 13. Evaluation of the tip shapes of nanometer size microelectrodes. J Electroanal Chem. 1992 Jul; 328(1-2):47-62.

[4] Edwards MA, Martin S, Whitworth AL, Macpherson JV, Unwin PR. Scanning electrochemical microscopy: principles and applications to biophysical systems. Physiol Meas. 2006 Dec;27(12):R63-R108.

[5] Nagy G, Nagy L. Scanning electrochemical microscopy: a new way of making electrochemical experiments. Fresenius J Anal Chem. 2000 Mar-Apr;366(6-7):735-44.

[6] Roberts WS, Lonsdale DJ, Griffiths J, Higson SPJ. Advances in the application of scanning electrochemical microscopy to bioanalytical systems. Biosens Bioelectron. 2007 Oct;23(3):301-18.

[7] Souto RM, Gonzalez-Garcia Y, Gonzalez S. Characterization of coating systems by scanning electrochemical microscopy: Surface topology and blistering. Prog Org Coat. 2009 Aug;65(4):435-9.

[8] de la Escosura-Muniz A, Ambrosi A, Merkoci A. Electrochemical analysis with nanoparticle-based biosystems. Trac-Trends Anal Chem. 2008 Jul-Aug;27(7):568-84.

[9] Amemiya S, Guo JD, Xiong H, Gross DA. Biological applications of scanning electrochemical microscopy: chemical imaging of single living cells and beyond. Anal Bioanal Chem. 2006 Oct;386(3):458-71.

[10] Amemiya S, Bard AJ, Fan FRF, Mirkin MV, Unwin PR. Scanning Electrochemical Microscopy. *Annual Review of Analytical Chemistry*. Palo Alto: Annual Reviews 2008:95-131.

[11] Wittstock G, Burchardt M, Pust SE, Shen Y, Zhao C. Scanning electrochemical microscopy for direct imaging of reaction rates. Angew Chem-Int Edit. 2007;46(10): 1584-617.

[12] Mirkin MV, Nogala W, Velmurugan J, Wang YX. Scanning electrochemical microscopy in the 21st century. Update 1: five years after. Phys Chem Chem Phys. 2011;13(48): 21196-212.

[13] Fulian Q, Fisher AC, Denuault G. Applications of the boundary element method in electrochemistry: Scanning electrochemical microscopy. J Phys Chem B. 1999 May; 103(21):4387-92.

[14] Fulian Q, Fisher AC, Denuault G. Applications of the boundary element method in electrochemistry: Scanning electrochemical microscopy, part 2. J Phys Chem B. 1999 May;103(21):4393-8.

[15] Szunerits S, Pust SE, Wittstock G. Multidimensional electrochemical imaging in materials science. Anal Bioanal Chem. 2007 Oct;389(4):1103-20.

[16] Hamou RF, Biedermann PU, Erbe A, Rohwerder M. Numerical simulation of probing the electric double layer by scanning electrochemical potential microscopy. Electrochim Acta. 2010 Jul;55(18):5210-22.

[17] Lu X, Wang Q, Liu X. Review: Recent applications of scanning electrochemical microscopy to the study of charge transfer kinetics. Anal Chim Acta. 2007 Oct;601(1): 10-25.

[18] Inaba M, Siroma Z, Funabiki A, Ogumi Z, Abe T, Mizutani Y, et al. Electrochemical scanning tunneling microscopy observation of highly oriented pyrolytic graphite surface reactions in an ethylene carbonate-based electrolyte solution. Langmuir. 1996 Mar;12(6):1535-40.

[19] Ibe JP, Bey PP, Brandow SL, Brizzolara RA, Burnham NA, Dilella DP, et al. On the electrochemical etching of tips for scanning tunneling microscopy. J Vac Sci Technol A-Vac Surf Films. 1990 Jul-Aug;8(4):3570-5.

[20] Macpherson JV, Unwin PR. Combined scanning electrochemical-atomic force microscopy. Anal Chem. 2000 Jan;72(2):276-85.

[21] Bain CD, Troughton EB, Tao YT, Evall J, Whitesides GM, Nuzzo RG. Formation of monolayer films by the spontaneous assembly of organic thiols from solution onto gold. J Am Chem Soc. 1989 Jan;111(1):321-35.

[22] Chen D, Li JH. Interfacial design and functionization on metal electrodes through self-assembled monolayers. Surf Sci Rep. 2006 Dec;61(11):445-63.

[23] Eckermann AL, Feld DJ, Shaw JA, Meade TJ. Electrochemistry of redox-active self-assembled monolayers. Coord Chem Rev. 2010 Aug;254(15-16):1769-802.

[24] Kiani A, Alpuche-Aviles MA, Eggers PK, Jones M, Gooding JJ, Paddon-Row MN, et al. Scanning electrochemical microscopy. 59. Effect of defects and structure on electron transfer through self-assembled monolayers. Langmuir. 2008 Mar;24(6):2841-9.

[25] Tao F, Bernasek SL. Understanding odd-even effects in organic self-assembled monolayers. Chem Rev. 2007 May;107(5):1408-53.

[26] Yamada H, Ogata M, Koike T. Scanning electrochemical microscope observation of defects in a hexadecanethiol monolayer on gold with shear force-based tip-substrate positioning. Langmuir. 2006 Aug 29;22(18):7923-7.

[27] Liu B, Bard AJ, Mirkin MV, Creager SE. Electron transfer at self-assembled monolayers measured by scanning electrochemical microscopy. J Am Chem Soc. 2004 Feb; 126(5):1485-92.

[28] Alizadeh V, Mousavi MF, Mehrgardi MA, Kazemi SH, Sharghi H. Electron transfer kinetics of cytochrome c immobilized on a phenolic terminated thiol self assembled monolayer determined by scanning electrochemical microscopy. Electrochim Acta. 2011 Jul;56(17):6224-9.

[29] Bar G, Rubin S, Taylor TN, Swanson BI, Zawodzinski TA, Chow JT, et al. Patterned self-assembled monolayers of ferrocene and methyl terminated alkanethiols on gold: A combined electrochemical, scanning probe microscopy, and surface science study. J Vac Sci Technol A-Vac Surf Films. 1996 May-Jun;14(3):1794-800.

[30] Salamifar SE, Mehrgardi MA, Kazemi SH, Mousavi MF. Cyclic voltammetry and scanning electrochemical microscopy studies of methylene blue immobilized on the self-assembled monolayer of n-dodecanethiol. Electrochim Acta. 2010 Dec;56(2): 896-904.

[31] Wittstock G, Hesse R, Schuhmann W. Patterned self-assembled alkanethiolate monolayers on gold. Patterning and imaging by means of scanning electrochemical microscopy. Electroanalysis. 1997 Jun;9(10):746-50.

[32] Zhang LM, Zuo RX, Liu XH, Lu XQ. The study on the self-assembled monolayer (SAMs) of porphyrin with different chain length by scanning electrochemical microscopy (SECM). Chin Chem Lett. 2006 May;17(5):661-4.

[33] Boldt FM, Baltes N, Borgwarth K, Heinze J. Investigation of carboxylic-functionalized and n-alkanethiol self-assembled monolayers on gold and their application as pH-sensitive probes using scanning electrochemical microscopy. Surf Sci. 2005 Dec; 597(1-3):51-64.

[34] Sanders W, Vargas R, Anderson MR. Characterization of carboxylic acid-terminated self-assembled monolayers by electrochemical impedance spectroscopy and scanning electrochemical microscopy. Langmuir. 2008 Jun;24(12):6133-9.

[35] Uosaki K, Wano H. Dynamic monitoring of electrochemical oxidative adsorption and reductive desorption of self-assembled monolayer of hexanethiol on Au(111) surface in KOH ethanol solution by in situ scanning tunneling microscopy. Abstr Pap Am Chem Soc. 2002 Aug;224:U449-U.

[36] Uosaki K, Wano H. Electrochemical formation and desorption of self-assembled monolayer of alkanethiol in ethanol solution monitored by in situ scanning tunneling microscopy. Abstr Pap Am Chem Soc. 2002 Apr;223:U413-U.

[37] Burshtain D, Mandler D. Studying the binding of Cd2+ by omega-mercaptoalkanoic acid self assembled monolayers by cyclic voltammetry and scanning electrochemical microscopy (SECM). J Electroanal Chem. 2005 Aug;581(2):310-9.

[38] Palecek E, Fojta M. Magnetic beads as versatile tools for electrochemical DNA and protein biosensing. Talanta. 2007 Dec;74(3):276-90.

[39] Quinn BM, Prieto I, Haram SK, Bard AJ. Electrochemical observation of a metal/insulator transition by scanning electrochemical microscopy. J Phys Chem B. 2001 Aug; 105(31):7474-6.

[40] Tel-Vered R, Bard AJ. Generation and detection of single metal nanoparticles using scanning electrochemical microscopy techniques. J Phys Chem B. 2006 Dec;110(50): 25279-87.

[41] Wijayawardhana CA, Wittstock G, Halsall HB, Heineman WR. Electrochemical immunoassay with microscopic immunomagnetic bead domains and scanning electrochemical microscopy. Electroanalysis. 2000 May;12(9):640-4.

[42] Wijayawardhana CA, Wittstock G, Halsall HB, Heineman WR. Spatially addressed deposition and imaging of biochemically active bead microstructures by scanning electrochemical microscopy. Anal Chem. 2000 Jan;72(2):333-8.

[43] Zhao C, Wittstock G. Scanning electrochemical microscopy for detection of biosensor and biochip surfaces with immobilized pyrroloquinoline quinone (PQQ)-dependent glucose dehydrogenase as enzyme label. Biosens Bioelectron. 2005 Jan;20(7):1277-84.

[44] Zhao CA, Wittstock G. Scanning electrochemical microscopy of quinoprotein glucose dehydrogenase. Anal Chem. 2004 Jun;76(11):3145-54.

[45] Wang YC, Hu R, Lin GM, Roy I, Yong KT. Functionalized Quantum Dots for Biosensing and Bioimaging and Concerns on Toxicity. ACS Appl Mater Interfaces. 2013 Apr;5(8):2786-99.

[46] Katz E, Willner I, Wang J. Electroanalytical and bioelectroanalytical systems based on metal and semiconductor nanoparticles. Electroanalysis. 2004 Jan;16(1-2):19-44.

[47] Zimin S, Vasin V, Gorlachev E, Buchin E, Naumov V. Investigations of PbSe layers after anodic electrochemical etching by scanning electron microscopy. In: Cantarero

A, Sailor M, Nassiopoulou A, Schmuki P, Canham L, eds. *Physica Status Solidi C: Current Topics in Solid State Physics*. Weinheim: Wiley-V C H Verlag Gmbh 2011.

[48] Liu GJ, Liu CY, Bard AJ. Rapid Synthesis and Screening of Zn(x)zCd(1-x)S(y)Se(1-y) Photocatalysts by Scanning Electrochemical Microscopy. J Phys Chem C. 2010 Dec; 114(49):20997-1002.

[49] Hutchings GJ, Brust M, Schmidbaur H. Gold - an introductory perspective. Chem Soc Rev. 2008 Sep;37(9):1759-65.

[50] Wain AJ. Imaging size effects on the electrocatalytic activity of gold nanoparticles using scanning electrochemical microscopy. Electrochim Acta. 2013 Mar;92:383-91.

[51] Sanchez-Sanchez CM, Vidal-Iglesias FJ, Solla-Gullon J, Montiel V, Aldaz A, Feliu JM, et al. Scanning electrochemical microscopy for studying electrocatalysis on shape-controlled gold nanoparticles and nanorods. Electrochim Acta. 2010 Nov;55(27): 8252-7.

[52] Sanchez-Sanchez CM, Solla-Gullon J, Vidal-Iglesias FJ, Aldaz A, Montiel V, Herrero E. Imaging Structure Sensitive Catalysis on Different Shape-Controlled Platinum Nanoparticles. J Am Chem Soc. 2010 Apr;132(16):5622-4.

[53] Markovic NM, Adzic RR, Vesovic VB. Structural effects in electrocatalysis - Oxygen reduction on the gold single-crystal electrodes with (110) and (111) orientations. J Electroanal Chem. 1984;165(1-2):121-33.

[54] Adzic RR, Markovic NM, Vesovic VB. Structural effects in electrocatalysis - Oxygen reduction on the Au(100) single-crystal electrode. J Electroanal Chem. 1984;165(1-2): 105-20.

[55] El-Deab MS, Sotomura T, Ohsaka T. Size and crystallographic orientation controls of gold nanoparticles electrodeposited on GC electrodes. J Electrochem Soc. 2005;152(1):C1-C6.

[56] Huang K, Anne A, Bahri MA, Demaille C. Probing Individual Redox PEGylated Gold Nanoparticles by Electrochemical-Atomic Force Microscopy. ACS Nano. 2013 May;7(5):4151-63.

[57] Wang J, Zhou FM. Scanning electrochemical microscopic imaging of surface-confined DNA probes and their hybridization via guanine oxidation. J Electroanal Chem. 2002 Nov;537(1-2):95-102.

[58] Wang J, Song FY, Zhou FM. Silver-enhanced imaging of DNA hybridization at DNA microarrays with scanning electrochemical microscopy. Langmuir. 2002 Aug;18(17): 6653-8.

[59] Turcu F, Schulte A, Hartwich G, Schuhmann W. Imaging immobilised ssDNA and detecting DNA hybridisation by means of the repelling mode of scanning electrochemical microscopy (SECM). Biosens Bioelectron. 2004 Nov;20(5):925-32.

[60] Turcu F, Schulte A, Hartwich G, Schuhmann W. Label-free electrochemical recognition of DNA hybridization by means of modulation of the feedback current in SECM. Angew Chem-Int Edit. 2004;43(26):3482-5.

[61] Carano M, Lion N, Abid JP, Girault HH. Detection of proteins on poly(vinylidene difluoride) membranes by scanning electrochemical microscopy. Electrochem Commun. 2004 Dec;6(12):1217-21.

[62] Carano M, Lion N, Girault HH. Copper staining/labeling and Scanning Electrochemical Microscopy readout of proteins on poly(vinylidene difluoride) membranes. Chimia. 2005;59(3):105-8.

[63] Carano M, Lion N, Girault HH. Detection of proteins on membranes and in microchannels using copper staining combined with scanning electrochemical microscopy. J Electroanal Chem. 2007 Jan;599(2):349-55.

[64] Cortes-Salazar F, Busnel JM, Li F, Girault HH. Adsorbed protein detection by scanning electrochemical microscopy. J Electroanal Chem. 2009 Oct;635(2):69-74.

[65] Glidle A, Yasukawa T, Hadyoon CS, Anicet N, Matsue T, Nomura M, et al. Analysis of protein adsorption and binding at biosensor polymer interfaces using X-ray photon spectroscopy and scanning electrochemical microscopy. Anal Chem. 2003 Jun; 75(11):2559-70.

[66] Kirchner CN, Szunerits S, Wittstock G. Scanning electrochemical microscopy (SECM) based detection of oligonucleotide hybridization and simultaneous determination of the surface concentration of immobilized oligonucleotides on gold. Electroanalysis. 2007 Jun;19(12):1258-67.

[67] Wilhelm T, Wittstock G. Analysis of interaction in patterned multienzyme layers by using scanning electrochemical microscopy. Angew Chem-Int Edit. 2003;42(20): 2247-50.

[68] Wilhelm T, Wittstock G. Generation of periodic enzyme patterns by soft lithography and activity imaging by scanning electrochemical microscopy. Langmuir. 2002 Nov; 18(24):9485-93.

[69] Chen PC, Chen RLC, Cheng TJ, Wittstock G. Localized Deposition of Chitosan as Matrix for Enzyme Immobilization. Electroanalysis. 2009 Apr;21(7):804-10.

[70] Wilhelm T, Wittstock G, Szargan R. Scanning electrochemical microscopy of enzymes immobilized on structured glass-gold substrates. Fresenius J Anal Chem. 1999 Sep-Oct;365(1-3):163-7.

[71] Wu ZQ, Jia WZ, Wang K, Xu JJ, Chen HY, Xia XH. Exploration of Two-Enzyme Coupled Catalysis System Using Scanning Electrochemical Microscopy. Anal Chem. 2012 Dec;84(24):10586-92.

[72] Wittstock G, Yu KJ, Halsall HB, Ridgway TH, Heineman WR. Imaging of immobilized antibody layers with scanning electrochemical microscopy. Anal Chem. 1995 Oct;67(19):3578-82.

[73] Le HQA, Sauriat-Dorizon H, Korri-Youssoufi H. Investigation of SPR and electrochemical detection of antigen with polypyrrole functionalized by biotinylated single-chain antibody: A review. Anal Chim Acta. 2010 Jul;674(1):1-8.

[74] Holmes JL, Davis F, Collyer SD, Higson SPJ. A new application of scanning electrochemical microscopy for the label-free interrogation of antibody-antigen interactions. Anal Chim Acta. 2011 Mar;689(2):206-11.

[75] Holmes JL, Davis F, Collyer SD, Higson SPJ. A new application of scanning electrochemical microscopy for the label-free interrogation of antibody-antigen interactions: Part 2. Anal Chim Acta. 2012 Sep;741:1-8.

[76] Wittstock G. Modification and characterization of artificially patterned enzymatically active surfaces by scanning electrochemical microscopy. Fresenius J Anal Chem. 2001 Jun;370(4):303-15.

[77] Lu XQ, Wang TX, Zhou XB, Li Y, Wu BW, Liu XH. Investigation of Ion Transport Traversing the "Ion Channels" by Scanning Electrochemical Microscopy (SECM). J Phys Chem C. 2011 Mar;115(11):4800-5.

[78] Kim J, Izadyar A, Nioradze N, Amemiya S. Nanoscale Mechanism of Molecular Transport through the Nuclear Pore Complex As Studied by Scanning Electrochemical Microscopy. J Am Chem Soc. 2013 Feb;135(6):2321-9.

[79] Wilburn JP, Wright DW, Cliffel DE. Imaging of voltage-gated alamethicin pores in a reconstituted bilayer lipid membrane via scanning electrochemical microscopy. Analyst. 2006;131(2):311-6.

[80] Zhan W, Bard AJ. Scanning electrochemical microscopy. 56. Probing outside and inside single giant liposomes containing Ru(bpy)(3)(2+). Anal Chem. 2006 Feb;78(3):726-33.

[81] Amemiya S, Ding ZF, Zhou JF, Bard AJ. Studies of charge transfer at liquid vertical bar liquid interfaces and bilayer lipid membranes by scanning electrochemical microscopy. J Electroanal Chem. 2000 Mar;483(1-2):7-17.

[82] Cannes C, Kanoufi F, Bard AJ. Cyclic voltammetry and scanning electrochemical microscopy of ferrocenemethanol at monolayer and bilayer-modified gold electrodes. J Electroanal Chem. 2003 Apr;547(1):83-91.

[83] Tsionsky M, Zhou JF, Amemiya S, Fan FRF, Bard AJ, Dryfe RAW. Scanning electrochemical microscopy. 38. Application of SECM to the study of charge transfer through bilayer lipid membranes. Anal Chem. 1999 Oct;71(19):4300-5.

[84] Burt DP, Cervera J, Mandler D, Macpherson JV, Manzanares JA, Unwin PR. Scanning electrochemical microscopy as a probe of Ag+ binding kinetics at Langmuir phospholipid monolayers. Phys Chem Chem Phys. 2005;7(15):2955-64.

[85] Slevin CJ, Liljeroth P, Kontturi K. Measurement of the adsorption of drug ions at model membranes by scanning electrochemical microscopy. Langmuir. 2003 Apr; 19(7):2851-8.

[86] Bergner S, Vatsyayan P, Matysik FM. Recent advances in high resolution scanning electrochemical microscopy of living cells - A review. Anal Chim Acta. 2013 May; 775:1-13.

[87] Li XM, Geng QH, Wang YY, Si ZK, Jiang W, Zhang XL, et al. Fabrication of active horseradish peroxidase micropatterns with a high resolution by scanning electrochemical Microscopy. Electroanalysis. 2007 Aug;19(16):1734-40.

[88] Roberts WS, Davis F, Collyer SD, Higson SPJ. Construction and interrogation of enzyme microarrays using scanning electrochemical microscopy - optimisation of adsorption and determination of enzymatic activity. Analyst. 2011;136(24):5287-93.

[89] Cougnon C, Gohier F, Belanger D, Mauzeroll J. In Situ Formation of Diazonium Salts from Nitro Precursors for Scanning Electrochemical Microscopy Patterning of Surfaces. Angew Chem-Int Edit. 2009;48(22):4006-8.

[90] Cougnon C, Mauzeroll J, Belanger D. Patterning of Surfaces by Oxidation of Amine-Containing Compounds Using Scanning Electrochemical Microscopy. Angew Chem-Int Edit. 2009;48(40):7395-7.

[91] Janin M, Ghilane J, Randriamahazaka H, Lacroix JC. Microelectrodes modification through the reduction of aryl diazonium and their use in scanning electrochemical microscopy (SECM). Electrochem Commun. 2009 Mar;11(3):647-50.

[92] Schwamborn S, Stoica L, Neugebauer S, Reda T, Schmidt HL, Schuhmann W. Local Modulation of the Redox State of p-Nitrothiophenol Self-Assembled Monolayers Using the Direct Mode of Scanning Electrochemical Microscopy. ChemPhysChem. 2009 May;10(7):1066-70.

[93] Coates M, Cabet E, Griveau S, Nyokong T, Bedioui F. Microelectrochemical patterning of gold surfaces using 4-azidobenzenediazonium and scanning electrochemical microscopy. Electrochem Commun. 2011 Feb;13(2):150-3.

[94] Yong KT, Swihart MT, Ding H, Prasad PN. Preparation of Gold Nanoparticles and their Applications in Anisotropic Nanoparticle Synthesis and Bioimaging. Plasmonics. 2009 Jun;4(2):79-93.

[95] Fedorov RG, Mandler D. Local deposition of anisotropic nanoparticles using scanning electrochemical microscopy (SECM). Phys Chem Chem Phys. 2013;15(8): 2725-32.

[96] Li F, Edwards M, Guo JD, Unwin PR. Silver Particle Nucleation and Growth at Liquid/Liquid Interfaces: A Scanning Electrochemical Microscopy Approach. J Phys Chem C. 2009 Mar;113(9):3553-65.

[97] Malel E, Colleran J, Mandler D. Studying the localized deposition of Ag nanoparticles on self-assembled monolayers by scanning electrochemical microscopy (SECM). Electrochim Acta. 2011 Aug;56(20):6954-61.

[98] Treichel DA, Mirkin MV, Bard AJ. Scanning electrochemical microscopy. 27. Application of a simplified treatment of an irreversible homogeneous reaction following electron-transfer to the oxidative dimerization of 4-nitrophenolate in acetonitrile. J Phys Chem. 1994 Jun;98(22):5751-7.

[99] Lefrou C, Cornut R. Analytical Expressions for Quantitative Scanning Electrochemical Microscopy (SECM). ChemPhysChem. 2010 Feb;11(3):547-56.

[100] Amphlett JL, Denuault G. Scanning electrochemical microscopy (SECM): An investigation of the effects of tip geometry on amperometric tip response. J Phys Chem B. 1998 Dec;102(49):9946-51.

[101] Sun P, Mirkin MV. Kinetics of electron-transfer reactions at nanoelectrodes. Anal Chem. 2006 Sep;78(18):6526-34.

[102] Wittstock G, Wilhelm T. Characterization and manipulation of microscopic biochemically active regions by scanning electrochemical microscopy (SECM). Anal Sci. 2002 Nov;18(11):1199-204.

[103] Sklyar O, Wittstock G. Numerical simulations of complex nonsymmetrical 3D systems for scanning electrochemical microscopy using the boundary element method. J Phys Chem B. 2002 Aug;106(30):7499-508.

[104] Sklyar O, Kueng A, Kranz C, Mizaikoff B, Lugstein A, Bertagnolli E, et al. Numerical simulation of scanning electrochemical Microscopy experiments with frame-shaped integrated atomic force microscopy-SECM probes using the boundary element method. Anal Chem. 2005 Feb;77(3):764-71.

[105] Sklyar O, Trauble M, Zhao CA, Wittstock G. Modeling steady-state experiments with a scanning electrochemical microscope involving several independent diffusing species using the boundary element method. J Phys Chem B. 2006 Aug;110(32):15869-77.